

Mapping Brain Circuitry with a Light Microscope

Pavel Osten MD, PhD,¹ and Troy W. Margrie, PhD^{2,3}

¹Cold Spring Harbor Laboratory
Cold Spring Harbor, New York

²Department of Neuroscience, Physiology and Pharmacology
University College London
London, United Kingdom

³Division of Neurophysiology
The MRC National Institute for Medical Research
Mill Hill, London, United Kingdom

Introduction

The beginning of the 21st century has seen a renaissance in light microscopy and anatomical tract tracing that is rapidly advancing our understanding of the form and function of neuronal circuits. The introduction of instruments for automated imaging of whole mouse brains, new cell-type-specific and transsynaptic tracers, and computational methods for handling the whole-brain datasets has opened the door to neuroanatomical studies at an unprecedented scale. In this chapter, we present an overview of the state of play and future opportunities in charting long-range and local connectivity in the entire mouse brain and in linking brain circuits to function.

Since the pioneering work of Camillo Golgi in the latter 19th century and Santiago Ramón Y Cajal at the turn of the last century (Golgi, 1873; Ramón Y Cajal, 1904), advances in light microscopy (LM) and neurotracing methods have been central to the progress in our understanding of anatomical organization in the mammalian brain. The discovery of the Golgi silver-impregnation method allowed the visualization of neuron morphology, providing the first evidence for cell-type-based and connectivity-based organization in the brain. The introduction of efficient neuroanatomical tracers in the second half of the 20th century greatly increased the throughput and versatility of neuronal projection mapping, which led to the identification of many anatomical pathways and circuits, and revealed the basic principles of hierarchical and laminar connectivity in sensory, motor, and other brain systems (Rockland and Pandya, 1979; Felleman and Van Essen, 1991).

The beginning of this century has seen a new period of method-driven renaissance in neuroanatomy, one that is distinguished by the focus on large-scale projects generating unprecedented amounts of anatomical data. Instead of the traditional “cottage industry” approach of studying one anatomical pathway at a time, the new projects aim to generate complete datasets—so-called projectomes and connectomes—that can be used by the scientific community as resources for answering specific experimental questions. These efforts range in scale and resolution from the macroscopic—studies of the human brain by magnetic resonance imaging (MRI), to the microscopic—dense neural circuit reconstructions of small volumes of brain tissue by electron microscopy (EM) (Craddock et al., 2013; Helmstaedter, 2013).

Advancements in LM methods, the focus of our review, are being applied to the mapping of point-to-

point connectivity between all anatomical regions in the mouse brain by means of sparse reconstructions of anterograde and retrograde tracers (Bohland et al., 2009). Taking advantage of the automation of LM instruments, powerful data processing pipelines, and combinations of traditional and modern viral-vector-based tracers, teams of scientists at Cold Spring Harbor Laboratory (CSHL), the Allen Institute for Brain Science (AIBS), and University of California, Los Angeles (UCLA), are racing to complete a connectivity map of the mouse brain—dubbed the “mesoscopic connectome”—which will provide the scientific community with online atlases for viewing entire anatomical datasets (Bohland et al., 2009). This chapter describes the rationale for mapping connectivity in the whole mouse brain at the mesoscale level by LM. These efforts demonstrate the transformative nature of today’s LM-based neuroanatomy and the astonishing speed with which large amounts of data can be disseminated online and have an immediate impact on research in neuroscience laboratories around the world.

As the mouse mesoscopic connectomes are being completed, it is clear that LM methods will continue to impact the evolution of biological research and specifically neuroscience: New transsynaptic viral tracers are being engineered to circumvent the need to resolve synapses, which has constrained the interpretation of cell-to-cell connectivity in LM studies. Also, new assays combining anatomical and functional measurements are being applied to bridge the traditional structure–function divide in the study of the mammalian brain. This chapter aims to provide an overview of today’s state of the art in LM instrumentation and to highlight the opportunities for progress, as well as the challenges that need to be overcome, in order to transform neuronal tracing studies into a truly quantitative science yielding comprehensive descriptions of long-range and local projections and connectivity at the level of whole mouse brains. We also discuss current strategies for the integration of anatomy and function in the study of mouse brain circuits.

Automated Light Microscopes for Whole-Brain Imaging

The field of neuroanatomy has traditionally been associated with labor-intensive procedures that greatly limited the throughput of data collection. Recent efforts to automate LM instrumentation have standardized and dramatically increased the throughput of anatomical studies. The main challenge for these methods is to maintain the rigorous quality of traditional neuroanatomical studies, resulting

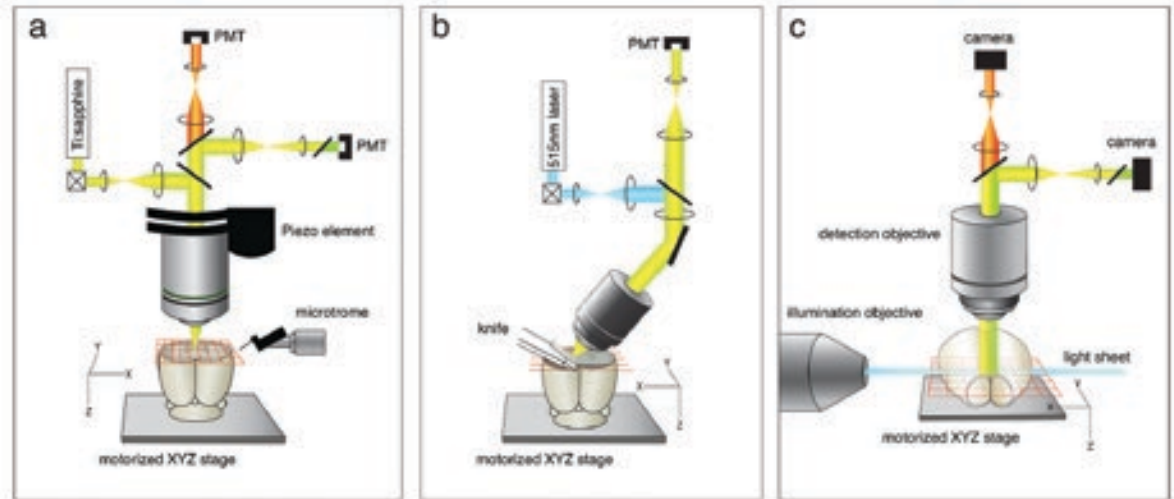


Figure 1. Whole-brain LM methods. **a**, STP tomography. Two-photon microscope is used to image the mouse brain in a coronal plane in a mosaic grid pattern and microtome sections off the imaged tissue. Piezo objective scanner can be used for z-stack imaging. Image adapted from Ragan et al. (2012), their Fig. 1a. **b**, fMOST. Confocal line-scan is used to image the brain as a 1 μm thin section cut by diamond knife. Image adapted from Gong et al. (2013), their Fig. 1a. **c**, LSFM. The cleared brain is illuminated from the side with the light sheet (blue) through an illumination objective (or cylinder lens [Dodt et al., 2007]) and imaged in a mosaic grid pattern from top. Image adapted from Niedworok et al. (2012), their Fig. 4g. In all instruments, the brain is moved under the objective on a motorized XYZ stage. PMT, photomultiplier tube.

from detailed visual analysis, careful data collection, and expert data interpretation.

There are currently two alternative approaches to automation of LM for imaging three-dimensional (3D) whole-brain datasets: one based on the integration of block-face microscopy and tissue sectioning, and the other based on light-sheet fluorescence microscopy (LSFM) of chemically cleared tissue. The first approach has been developed for wide-field imaging, line-scan imaging, and confocal and two-photon microscopy (Odgaard et al., 1990; Ewald et al., 2002; Tsai et al., 2003; Sands et al., 2005; Ragan et al., 2007; Mayerich et al., 2008; Li et al., 2011; Ragan et al., 2012; Gong et al., 2013). Common to all these instruments is the motorized movement of the sample under the microscope objective for top-view mosaic imaging, followed by mechanical removal of the imaged tissue before the next cycle of interleaved imaging and sectioning steps (Figs. 1a, b). Because the objective is always near the tissue surface, it is possible to use high numerical aperture (NA) lenses to achieve submicron resolution close to the diffraction limits of LM.¹

Three instruments have been designed that combine two-photon microscopy (Denk et al., 1990) followed by tissue sectioning by either ultra-short laser pulses in all-optical histology (Tsai et al., 2003), milling

machine in two-photon tissue cytometry (Ragan et al., 2007), or vibrating blade microtome in serial two-photon (STP) tomography (Ragan et al., 2012) (Fig. 1a). Whereas in both all-optical histology and two-photon tissue cytometry the sectioning obliterates the imaged tissue, the integration of vibratome-based sectioning in STP tomography allows the collection of the cut tissue for further analysis by, for example, immunohistochemistry (see Current Challenges and Opportunities for Whole-Brain LM Methods, below). In addition, the tissue preparation by simple formaldehyde fixation and agar embedding in STP tomography has minimal detrimental effects on fluorescence and brain morphology. This makes STP tomography applicable to a broad range of neuroanatomical projects utilizing genetically encoded fluorescent protein-based tracers, which are sensitive to fixation, dehydration, and tissue clearing conditions. This method is also versatile in terms of the mode and resolution of data collection. For example, imaging the mouse brain as a dataset of 280 serial coronal sections, evenly spaced at 50 μm and at xy resolution 1 μm , takes ~ 21 h and generates a brain atlas-like dataset

¹Tsai et al. pioneered the approach of serial imaging by two-photon microscopy and tissue sectioning for *ex vivo* collection of neuronanatomical data. Ragan et al. (2012) introduced the method of STP tomography and demonstrated its use for anterograde and retrograde tracing in the mouse brain. Gong et al. (2013) demonstrated the first long-range tracing of individual axons in the mouse brain by the fluorescence-MOST (fMOST) method.

of ~70 gigabytes (GB). A complete visualization can be achieved by switching to 3D scanning of z-volume stacks between the mechanical sectioning steps, which allows the entire mouse brain to be imaged, for instance, at 1 μm xy and 2.5 μm z resolution in ~8 d, generating ~1.5 terabytes (TB) of data (Ragan et al., 2012). The instrument is commercially available from TissueVision (Cambridge, MA). The AIBS is using this methodology for its Mouse Connectivity project (see Mesoscopic Connectivity-Mapping Projects, below).

Two instruments have been designed to combine bright-field line-scan imaging and ultra-microtome sectioning of resin-embedded tissue into methods named knife-edge scanning microscopy (KESM) (Mayerich et al., 2008) and micro-optical sectioning tomography (MOST) (Li et al., 2011) (Fig. 1b). The latter was used to image Golgi-stained mouse brain at $0.33 \times 0.33 \times 1.0 \mu\text{m}$ x-y-z resolution, generating >8 TB of data in ~10 d (Mayerich et al., 2008; Li et al., 2011). The MOST instrument design was also recently built for fluorescent imaging (fMOST) by confocal laser scanning microscopy, with the throughput of one mouse brain at 1.0 μm voxel resolution in ~19 d (Gong et al., 2013). KESM imaging is now also available as a commercial service from 3Scan (San Francisco, CA).

The second, alternative, approach for automated whole-brain imaging is based on LSFM, also known as selective-plane illumination microscopy or SPIM (Huisken et al., 2004) and ultramicroscopy (Dodt et al., 2007) (Fig. 1c). Dodt et al. (2007) was the first to demonstrate the use of LSFM for imaging the entire mouse brain. This approach allows fast imaging of chemically cleared “transparent” mouse brains without the need for mechanical sectioning (Dodt et al., 2007; Niedworok et al., 2012), but at least until now, with some trade-offs for anatomical tracing applications. The chemical clearing procedures reduce the signal of fluorescent proteins, but this problem appears to be solved by a new hydrogel-based tissue transformation and clearing method called CLARITY (Chung et al., 2013; Chung and Deisseroth, 2013) (See the Short Course chapters “Advanced CLARITY Methods for Rapid and High-Resolution Imaging of Intact Tissues” by R. Tomer and K. Deisseroth and “CLARITY and Beyond: Tools for Integrated Brain Mapping” by K. Chung.) The spatial resolution of LSFM for the mouse brain has also been limited by the requirement for large field-of-view objectives with low power and low NA that were used for the

visualization of the whole brain (Dodt et al., 2007; Leischner et al., 2009). However, new objectives with long working distance (WD) and high NA, such as 8 mm WD/0.9 NA objective from Olympus, promise to enable LSFM of the whole mouse brain at submicron resolution. If necessary, LSFM can also be combined with one of several forms of structured illumination (SI) to reduce out-of-focus background fluorescence and improve contrast (Kalchmair et al., 2010; Keller et al., 2010; Mertz and Kim, 2010). Taken together, these modifications are likely to enhance the applicability of LSFM to anterograde tracing of thin axons at high resolution in the whole mouse brain, as done by STP tomography in the AIBS Mouse Connectivity project (see Mesoscopic Connectivity-Mapping Projects, below) and by fMOST in a recent report (Gong et al., 2013).

In addition, LSFM is well suited for retrograde tracing in the mouse brain, which relies on detection of retrogradely fluorescently labeled neuronal somas that are typically >10 μm in diameter. Such application was recently demonstrated for mapping retrograde connectivity of granule cells of the mouse olfactory bulb (Niedworok et al., 2012) using rabies viruses that achieve high levels of fluorescent protein labeling (Wickersham et al., 2007a, b). (Wickersham et al., 2007a, described a genetically modified rabies virus designed to specifically label direct presynaptic input onto a given cell population.)

Mesoscopic Connectivity-Mapping Projects

The labeling of neurons and subsequent neuroanatomical tract tracing by LM methods has been used for more than a century to interrogate the anatomical substrate of information transmission in the brain. Throughout those years, the credo of neuroanatomy, “The gain in brain is mainly in the stain,” meant to signify that progress was made mainly through the development of new anatomical tracers. Yet despite the decades of neuroanatomical research, the laborious nature of tissue processing and data visualization kept the progress in our knowledge of brain circuitry at a disappointingly slow pace (Bohland et al., 2009). Today, neuroanatomy stands to greatly benefit from the application of high-throughput automated LM instruments and powerful informatics tools for the analysis of mouse brain data (Ng et al., 2009; Jones et al., 2011). The high-resolution capacity these LM methods afford, and the fact that an entire brain dataset can be captured, makes these systems well suited for systematic

NOTES

charting of the spatial profile and connectivity of populations of neurons and even individual cells projecting over long distances.

The pioneering effort in the field of anatomical projects applied at the scale of whole animal brains was the Allen Mouse Brain Atlas of Gene Expression, which catalogued *in situ* hybridization maps of more than 20,000 genes in an online 3D digital mouse brain atlas (Lein et al., 2007; Dong, 2008; Ng et al., 2009). (Lein et al., 2007, pioneered large-scale LM-based whole-brain anatomy and introduced the Allen Mouse Brain Atlas and online data portal.)

The proposal by a consortium of scientists led by Partha Mitra (CSHL) to generate similar LM-based atlases of “brainwide neuroanatomical connectivity” in several animal models (Bohland et al., 2009) has in short time spurred three independent projects, each promising to trace all efferent and afferent anatomical pathways in the mouse brain. The Mitra team’s Mouse Brain Architecture Project (<http://brainarchitecture.org>) at CSHL aims to image >1000 brains; the Allen Mouse Brain Connectivity Atlas project (<http://connectivity.brain-map.org>), led by Hongkui Zeng at AIBS, plans for >2000 brains; and the Mouse Connectome Project (www.mouseconnectome.org), led by Hong-Wei Dong at UCLA, plans for 500 brains, each brain injected with 4 tracers. While the CSHL and UCLA projects use automated wide-field fluorescence microscopy (Hamamatsu Nanoscope 2.0 [Hamamatsu Photonics, Hamamatsu City, Japan] and Olympus VS110) to image manually sectioned brains, the Mouse Connectivity project at the AIBS is being done entirely by STP tomography (Ragan et al., 2012).

The main complementary strength of these efforts, however, comes from the broad range of tracers used. Given that each tracer has its own advantages and problems (Lanciego and Wouterlood, 2011), the information derived from all three projects will ensure generalizable interpretation of the projection results throughout the brain. The CSHL group uses a combination of traditional anterograde and retrograde tracers, fluorophore-conjugated dextran amine (BDA) (Glover et al., 1986), and cholera toxin B (CTB) subunit (Llewellyn-Smith et al., 2000), respectively, which are complemented by a combination of viral-vector-based tracers, green fluorescent protein (GFP)-expressing adeno-associated virus (AAV) (Grinevich et al., 2005) for anterograde tracing (Fig. 2a), and modified rabies virus (Wickersham et al., 2007a) for retrograde tracing. Although the virus-based methods are less tested, they offer advantages in terms of the

brightness of labeling and the possibility of cell-type-specific targeting using Cre-dependent viral vectors (Atasoy et al., 2008) and transgenic lines expressing the Cre recombinase enzyme under the control of cell-type-specific promoters (Madisen et al., 2010, 2012; Taniguchi et al., 2011). The AIBS team uses solely anterograde tracing by AAV-GFP viruses (Harris et al., 2012) (Fig. 2b), in many cases taking advantage of Cre driver mouse lines for cell-type-specific labeling. Finally, the team at UCLA is using a strategy of two injections per brain, each with a mix of anterograde and retrograde tracers (Thompson and Swanson, 2010), CTB together with *Phaseolus vulgaris* leucoagglutinin (PHA-L) (Gerfen and Sawchenko, 1984), and FluoroGold (FG) (Naumann et al., 2000) together with BDA (Reiner et al., 2000; Thompson and Swanson, 2010). This approach has an added advantage because it allows direct visualization of the convergence of inputs and outputs from across different areas in one brain (Conte et al., 2009; Thompson and Swanson, 2010; Hintiryan et al., 2012).

The unprecedented amounts of data being collected by these projects means that the significant person-hours historically spent performing microscopy have largely shifted toward data analysis. The first step of such data analysis comprises the compilation of the serial section images for viewing as whole-brain datasets at resolutions beyond the minimum geometric volume of the neuronal structures of interest: somas for retrograde and axons for anterograde tracing. All three projects offer a convenient way to browse the datasets online, including high-resolution zoom-in views that in most cases are sufficient for visual determination of labeled somas and axons. Importantly, all three projects use the Allen Mouse Brain Atlas for the registration of the coronal sections, which will provide significant help in the cross-validation of results obtained from the different tracers. The Allen Mouse Brain Connectivity Atlas website (<http://connectivity.brain-map.org/static/brainexplorer>) also offers the option to view the data after projection segmentation, which selectively highlights labeled axons, as well as in 3D in the Brain Explorer registered to the Allen Mouse Brain Atlas (Sunkin et al., 2013) (Fig. 2b).

The second step of data analysis requires the development of informatics methods for quantitation of the datasets, which will facilitate the interpretation of the online available data. The Allen Mouse Brain Connectivity Atlas online tools allow the user to search the projections between injected regions and display the labeled pathways as tracks in 3D in the Brain Explorer. The CSHL and UCLA connectomes can

currently be viewed online as serial section datasets. The data from the Cre driver mouse lines in the AIBS project provide a unique feature of cell-type specificity for the interpretation of the anterograde projections. The main strength of the CSHL and UCLA efforts lies in the multiplicity of the anatomical tracers utilized. The use of multiple retrograde tracers in particular will yield useful information, since retrogradely labeled somas ($>10\ \mu\text{m}$ in diameter) are easier to quantitate than thin ($<1\ \mu\text{m}$) axon fibers. These experiments will also provide an important comparison between the traditional CTB and FluoroGold tracers and the rabies-virus tracer that is also being used in transsynaptic labeling (see below), but is less studied and may show some variation in transport affinity at different types of synapses.

In summary, the LM-based mesoscopic mapping projects are set to transform the study of the circuit wiring of the mouse brain by providing online access to whole-brain datasets from several thousand injections of anterograde and retrograde tracers. The informatics

tools being developed to search the databases will greatly aid in parsing the large amounts of data and in accessing specific brain samples for detailed scholarly analyses by the neuroscience community.

Mapping Connectivity Using Transsynaptic Tracers

In contrast to EM methods, which provide a readout of neuronal connectivity with synapse resolution over small volumes of tissue, the whole-brain LM methods permit the assessment of projection-based connectivity between brain regions and, in some cases, between specific cell types in those regions, but without the option to visualize the underlying synaptic contacts. Transsynaptic viruses that cross either multiple or single synapses can help circumvent the requirement to confirm connectivity at the EM resolution, since such connectivity may be inferred from the known direction and mechanism of spread of the transsynaptic tracer. Transsynaptic tracers based on rabies (RV), pseudorabies (PRV), and herpes simplex (HSV) viruses, which repeatedly cross

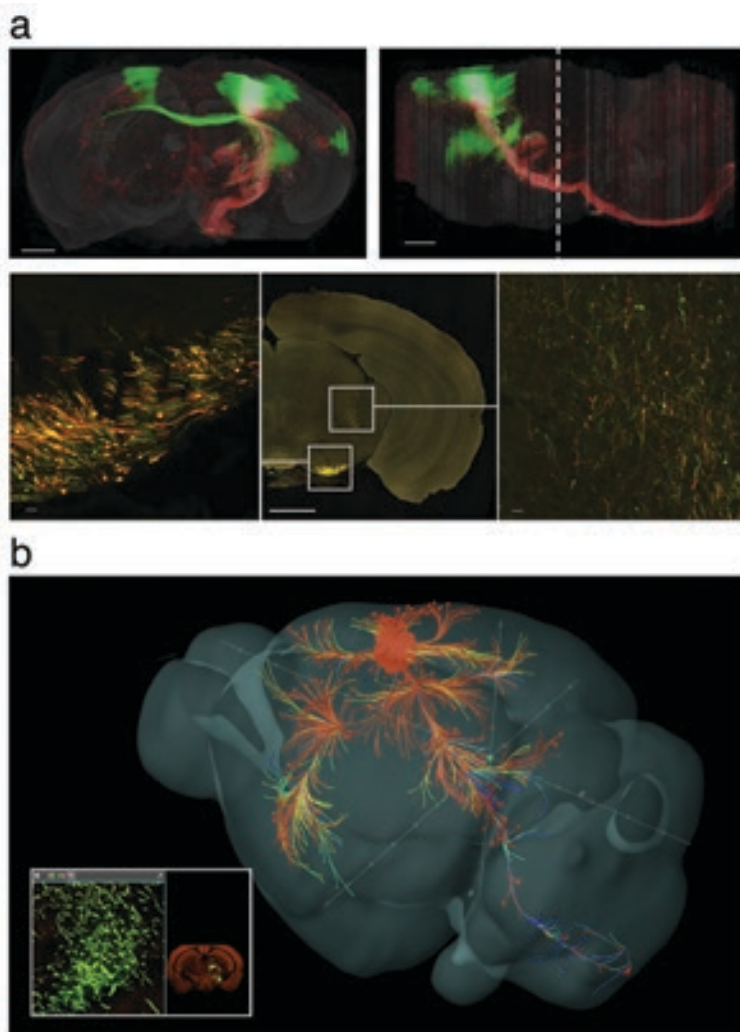


Figure 2. Primary motor cortex (MOp) projection maps. **a**, Mouse Brain Architecture (<http://brainarchitecture.org>) data of AAV-GFP injected into the supragranular layers and AAV-red fluorescent protein (RFP) injected in the infragranular layers (F. Mechler and P. Mitra, CSHL, unpublished observations). Top panels, Frontal (left) and lateral (right) views of the volume-rendered brain. Scale bars, 1000 μm . Bottom panels, High-zoom views of the regions highlighted in the central image. Left, Axonal fibers in the cerebral peduncle; Right, Projections to the midbrain reticular nucleus. Scale bars, 20 μm . **b**, Mouse Connectivity (<http://connectivity.brain-map.org>) data of a similar AAV-GFP injection show the MOp projectome reconstructed in the Allen Brain Explorer (Sunken et al., 2013; H. Zeng, AIBS, unpublished observations). Lower left inset, High-zoom view and coronal section overview of projections in the ventral posteromedial nucleus of the thalamus (VPM).

NOTES

synaptic connections in a retrograde or anterograde direction, are powerful tools for elucidating multistep pathways both up and downstream from the starter cell population (Song et al., 2005; Ekstrand et al., 2008; Ugolini, 2010). Furthermore, modified transsynaptic RVs have been developed that are restricted in their spread to a single synaptic jump and thus can be used to identify monosynaptic connections onto and downstream of specific neuronal populations and even individual cells (Wickersham et al., 2007a; Callaway, 2008; Marshel et al., 2010; Arenkiel et al., 2011; Miyamichi et al., 2011; Rancz et al., 2011; Wickersham and Feinberg, 2012; Takatoh et al., 2013).

RV spreads from the initially infected cells in a transsynaptic retrograde manner (Finke and Conzelmann, 2005; Ugolini, 2010). RV infection does not occur via spurious spread or uptake by fibers of passage and, since it cannot cross via electrical synapses, it is an effective tool for unidirectional anatomical tracing (Ugolini, 1995). In the modified RV system, the infection can also be cell-type-targeted by encapsulating the glycoprotein-deficient RV with an avian virus envelope protein (SAD- Δ G-EnvA). This restricts infection to only those cells that express an avian tumor virus receptor A gene (TVA), which is natively found in birds but not in mammals (Young et al., 1993; Federspiel et al., 1994). Thus, the delivery of vectors driving the expression of both TVA and RV-glycoprotein (RV-G) into a single cell (Wickersham et al., 2007b; Marshel et al., 2010; Rancz et al., 2011) (see Integrating Brain Anatomy and Function, below) or a specific population of cells (Wall et al., 2010; Miyamichi et al., 2011) ensures that only the targeted cell or cells will (1) be susceptible to initial infection and (2) provide the replication-incompetent virus with RV-G required for transsynaptic infection (Eteessami et al., 2000). In this system, the virus can spread from the primarily infected cell(s) to the presynaptic input cells, which become labeled by the fluorescent protein expression. However, because the presynaptic cells do not express RV-G (Wickersham et al., 2007b), the virus cannot spread further. This approach thus allows the discovery of the identity and location of the upstream input network relative to a defined population of neurons (Arenkiel et al., 2011; Takatoh et al., 2013).²

Brain-region and cell-type specificity for mapping connectivity by the modified RV system can be achieved by using a Cre recombinase-dependent helper virus driving expression of TVA and RV-G and transgenic mouse lines that express Cre in specific cell types or cortical layers (Madisen et al.,

2010; Wall et al., 2010; Taniguchi et al., 2011). This strategy is particularly useful for brain regions comprising many different cell types that could not otherwise be selectively targeted. Moreover, the engineering of other neurotropic transsynaptic viruses is adding new tools for anatomical tracing, including Cre-dependent anterograde tracers based on a modified H129 strain of HSV (Lo and Anderson, 2011) and vesicular stomatitis virus (Beier et al., 2011), and retrograde tracers based on a modified PRV (H. Oyibo and A. Zador, CSHL, personal communication). The use of retrograde and anterograde transsynaptic viruses, in combination with whole-brain LM methods, thus promises to afford unprecedented access to the upstream and downstream connectivity of specific cell types in the mouse brain.

Current Challenges and Opportunities for Whole-Brain LM Methods

As highlighted above, LM instruments for whole-brain imaging are expected to make a significant contribution in large-scale projects that focus on anatomical connectivity at the level of the whole mouse brain. It has also become clear that the use of these instruments will have an impact in many experimental applications in different neuroscience laboratories. It is therefore imperative that there exist broadly applicable image processing, warping, and analytical tools that will facilitate data sharing and across-laboratory collaboration and validation in future neuroscience studies focusing on, for example, mapping whole-brain anatomical changes during development and in response to experience.

One practical problem arising from the choice to scan entire mouse brains at high resolution relates to the handling of large datasets (up to several TB per brain), which necessitates automated analytical pipelining. STP tomography is currently the most broadly used method among the whole-brain LM instruments, and there are freely available informatics tools for compiling STP tomography image stacks and viewing them as 3D data, including algorithms that automate seamless stitching (Ragan et al., 2012). Another key challenge for charting the distribution of the labeled elements in the whole mouse brain is the process of accurate registration

²Rancz et al. (2011) were the first to combine intracellular neuronal recording with DNA delivery. The authors used this method to map the synaptic function of a single cell *in vivo* and then target RV-based retrograde labeling of the cells' synaptic input. Marshel et al. (2010) described an electroporation method for single-cell delivery of DNA for targeted infection of modified RV.

of the individual brain datasets onto an anatomical reference atlas. To this end, scientists at AIBS have generated the open-source, segmented Allen Mouse Brain Atlas for the adult C57BL/6 mouse (Lein et al., 2007; Dong, 2008; Ng et al., 2009; Sunkin et al., 2013), which is also available for registration of datasets generated by STP tomography (Figs. 2b, 4). In addition, the so-called Waxholm space (WHS) for standardized digital atlasing (Hawrylycz et al., 2011) allows comparisons of registered mouse brain data using multiple brain atlases, including the Allen Mouse Brain Atlas, the digital Paxinos and Franklin Mouse Brain Atlas (Paxinos and Franklin, 2004), and several MRI reference mouse brains. The continuing development of the WHS and other online data analysis platforms (Moene et al., 2007; Swanson and Bota, 2010; Jones et al., 2011) will be essential for making standardized comparisons of mouse brain data collected by different laboratories using different instruments.

The completion of the three mesoscopic connectome projects in the next several years will yield a comprehensive map of point-to-point connectivity between anatomical regions in the mouse brain (Bohland et al., 2009). Determining the cell-type identity of the neurons sending and receiving the connections in the brain regions will be essential for interpreting the function of the brainwide neural circuits. Immunohistochemical analyses of labeled circuits have proven invaluable for ascertaining the identity of specific classes of neurons (Klausberger and Somogyi, 2008; O'Rourke et al., 2012; Defelipe et al., 2013) and synaptic connections (Callaway, 2008; Emes and Grant, 2012). The combination of immunohistochemical analysis by array tomography (Micheva and Smith, 2007; Micheva et al., 2010) and anatomical tracing by the whole-brain LM instruments promises to be particularly powerful, since it will bring together two largely automated methodologies with complementary focus on synaptic and mesoscopic connectivity, respectively. STP tomography outputs sectioned tissue (typically, 50- μm -thick sections [Ragan et al., 2012]), which can be further resectioned, processed and reimaged by array tomography for integrating cell-type-specific information into the whole-brain datasets. Industrial-level automation of slice capture and immunostaining can be developed to minimize manual handling and enhance the integration of immunohistochemistry and STP tomography. In addition, sectioning and immunostaining can be applied to LSFM-imaged mouse brains (Niedworok et al., 2012).

A related, cell-type-focused application of whole-brain LM imaging will be to quantitatively map the

distribution (the cell counts) of different neuronal cell types in all anatomical regions in the mouse brain. Several such cell-count-based anatomical studies have been done previously at smaller scales, revealing, for example, cell densities with respect to cortical vasculature (Tsai et al., 2009) or the density of neuronal cell types per layers in a single cortical column (Meyer et al., 2010, 2011; Oberlaender et al., 2012). Using the whole-brain LM methods, a comprehensive anatomical atlas of different GABAergic inhibitory interneurons (Petilla Interneuron Nomenclature Group et al., 2008) can now be generated by imaging cell-type-specific Cre knock-in mouse lines (Madisen et al., 2010; Taniguchi et al., 2011) crossed with Cre-dependent reporter mice expressing nuclear GFP. These and similar datasets for other neuronal cell types will complement the mesoscopic brain region connectivity data and help the interpretation of the immunohistochemistry data by providing a reference for total numbers of specific cell types per anatomical brain region.

Integrating Brain Anatomy and Function

The anterograde, retrograde, and transsynaptic tracing approaches described above will yield the structural scaffold of anatomical projections and connections throughout the mouse brain. However, such data will not be sufficient to identify how specific brain regions connect to form functional circuits driving different behaviors. Bridging whole-brain structure and function is the next frontier in systems neuroscience, and the development of new technologies and methods will be crucial in achieving progress.

The structure–function relationship of single neurons can be examined by *in vivo* intracellular delivery of the DNA vectors required for targeting and driving transsynaptic virus expression via patch pipettes in loose cell-attached mode for electroporation (Marshel et al., 2010) or via whole-cell recording (Rancz et al., 2011) (Fig. 3). Used in combination with two-photon microscopy, this single-cell delivery technique may also be targeted at fluorescently labeled neurons of specific cell types (Margrie et al., 2003; Kitamura et al., 2008; Marshel et al., 2010). The whole-cell method is particularly informative, since its intracellular nature permits recording the intrinsic biophysical profile of the target cell, which, in turn, may reflect its functional connectivity status within the local network (Angelo et al., 2012). In addition, by recording sensory-evoked inputs, it is possible to compare single-cell

NOTES

synaptic receptive fields with anatomical local and long-range connectivity traced by LM methods (Rancz et al., 2011). This combinatorial approach, involving single-cell electrophysiology and genetic manipulation designed for connection mapping, makes it possible to test long-standing theories regarding the extent to which emergent features of sensory cortical function manifest via specific wiring motifs (Reid, 2012).

As has recently been achieved for serial EM-based reconstruction (Bock et al., 2011; Briggman et al., 2011), it will also be valuable to functionally characterize larger local neuronal populations for registration against LM-based connectivity data. In this sense, genetically encoded calcium indicators (GECIs), which permit physiological characterization of neuronal activity in specific cell types (Mank et al., 2008; Wallace et al., 2008; Akerboom et al., 2012), alongside viral vectors for transsynaptic labeling and LM-based tracing, will play critical complementary roles. Large-volume *in vivo* two-photon imaging of neuronal activity before *ex vivo* whole-brain imaging will establish the extent to which connectivity patterns relate to function (Ko et al., 2011) at the level of single cells and local and long-range circuits. Interpolation of such experiments will rely on the ability to cross-register *in vivo* functional imaging with complete *ex vivo* LM

connectivity data. Preliminary experiments (already hinting at the spatial spread of monosynaptic connectivity of individual principal cortical cells) suggest that the combination of functional imaging with traditional anatomical circuit reconstruction may be feasible only at the local network level, where connection probability is the highest (Thomson et al., 2002; Holmgren et al., 2003; Song et al., 2005). Given the broad, sparse expanse of connectivity in most brain regions—and especially in cortical areas—high-throughput whole-brain LM methods will be imperative for complete anatomical circuit reconstruction of the functionally characterized local networks.

The amalgamation of whole-brain LM and physiological methods for single neurons and small networks offers a powerful means to study the mouse brain. A promising application of this approach will be to trace the synaptic circuits of neurons functionally characterized in head-fixed behaving animals engaged in tasks related to spatial navigation, sensorimotor integration, and other complex brain functions (Harvey et al., 2009, 2012; Huber et al., 2012). (Harvey et al., 2009, introduced the method of physiological recording in head-restrained mice on a spherical treadmill performing spatial tasks in virtual environment.) This research will lead to the generation of whole-brain structure–function

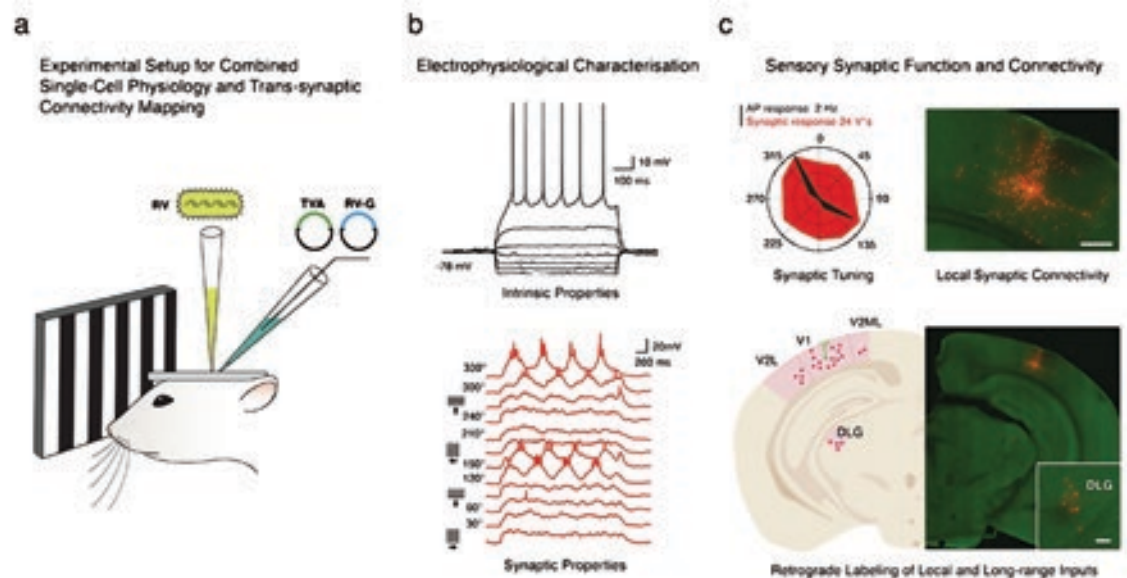


Figure 3. Mapping the function and connectivity of single cells in the mouse brain *in vivo*. **a**, Patch pipettes (with internal solutions containing DNA vectors used to drive the expression of the TVA and RV-G proteins) are used to perform a whole-cell recording of the intrinsic and sensory-evoked synaptic properties of a single layer 5 neuron in primary visual cortex. **b**, Following the recording, the encapsulated modified RV is injected into the brain in proximity to the recorded neuron. **c**, After a period of ≤ 12 d that ensures retrograde spread of the modified RV from the recorded neuron, the brain is removed and imaged for identification of the local and long-range presynaptic inputs underlying the tuning of the recorded neuron to the direction of visual motion (polar plot). Top and bottom scale bars, 300 μ m and 50 μ m, respectively. Images modified from Rancz et al. (2011), their Fig. 4. AP, action potential; DLG, dorsal lateral geniculate.

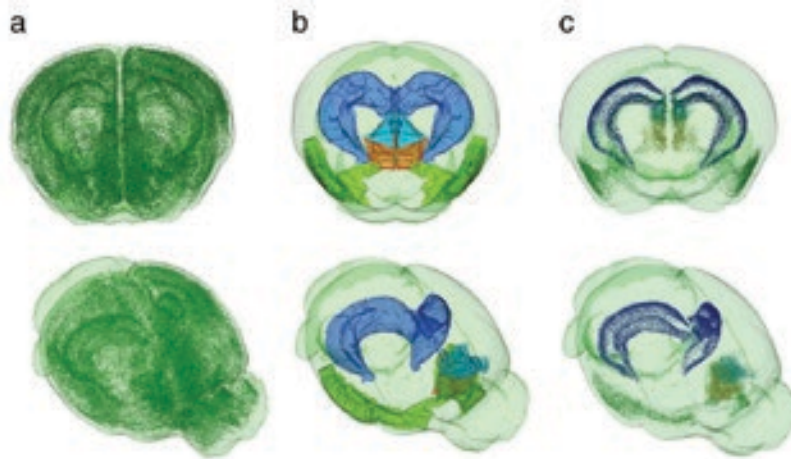


Figure 4. Imaging *c-fos* induction as a means to map whole-brain activation. **a**, 3D visualization of 367,378 *c-fos*-GFP cells detected in 280 coronal sections of an STP tomography dataset of a mouse brain after novelty exploration. **b**, Examples of anatomical segmentation of the brain volume with the Allen Mouse Brain Reference Atlas labels (Sunkin, et al., 2013) modified for the 280-section STP tomography datasets: hippocampus (blue), prelimbic (aqua blue), infralimbic (orange), and piriform (green) cortex. **c**, Visualization of *c-fos*-GFP cells in the hippocampus (38,170 cells), prelimbic (3305 cells), infralimbic (3827 cells), and piriform (10,910 cells) cortex (P. Osten, Y. Kim, and K. Umadevi Venkataraju, CSHL, unpublished observations).

hypotheses for specific behaviors, which can then be tested for causality by optogenetic methods targeted to the identified cell types and brain regions (Fenno et al., 2011). Furthermore, the LM, physiological, and optogenetic methods can be applied to interrogate entire brain systems in large-scale projects, as is currently being done for the mouse visual cortex in an effort led by Christof Koch and R. Clay Reid at AIBS (Koch and Reid, 2012).

Finally, the neuroscience community has begun to discuss the feasibility of mapping activity at cellular resolution in whole brains and linking the identified activity patterns to brain anatomy (Alivisatos et al., 2013). Today, such experiments are possible in small, transparent organisms, as was demonstrated by two-photon microscopy and LSFM-based imaging of brain activity in larval zebrafish expressing the calcium indicator GCaMP (Ahrens et al., 2012; Akerboom et al., 2012; Ahrens and Keller, 2013). Understandably, however, LM-based approaches will not be useful for *in vivo* whole-brain imaging in larger, nontransparent animals; thus, the invention of new, disruptive technologies will likely be needed to achieve the goal of real-time brain activity mapping at cellular resolution in, for example, the mouse. On the other hand, LM methods can be used to map patterns of whole-brain activation indirectly, by post hoc visualization of activity-induced expression of immediate early genes (IEGs), such as *c-fos*, *Arc*, or *Homer 1a* (Herrera and Robertson, 1996). Transgenic fluorescent IEG-reporter mice, like *c-fos*-GFP or *Arc*-GFP mice (Barth et al., 2004; Reijmers et al., 2007; Grinevich et al., 2009), can be trained in a

specific behavior, their brains subsequently imaged *ex vivo*, and the exact distribution of GFP-positive neurons mapped and analyzed by computational methods (Fig. 4). In this approach, a statistical analysis of the counts of GFP-labeled neurons can be used to identify brain regions and cell types activated during behaviors, but without providing any information on the temporal sequence of brain region activation or the firing patterns of the activated cells. However, the development of more sensitive (e.g., fluorescent RNA-based) methods may allow calibration of the cellular signal with respect to the temporal window and the pattern of activity related to the IEG induction. Such calibration would significantly enhance the power of LM-based whole-brain IEG mapping, which, in combination with the connectomic data, could then be used to begin to build cellular resolution models of function-based whole-brain circuits.

Conclusion

The advances in automated LM methods, anatomical tracers, physiological methods, and informatics tools have begun to transform our understanding of the circuit wiring in the mouse brain. The focus on the mouse as an animal model is, of course, not accidental. In addition to the generation of cell-type-specific knock-in mouse lines (Madisen et al., 2010, 2012; Taniguchi et al., 2011) that allow the study of specific neuronal populations in the normal brain, mouse genetics are used in hundreds of laboratories to model gene mutations linked to heritable human disorders, including complex cognitive disorders such as autism and schizophrenia. Without doubt,

NOTES

understanding the relationships between brain structure and function in the genetic mouse models will be crucial to understanding the underlying brain circuit mechanisms of these disorders. The toolbox of LM methods described here, and the continuing development of new methods, promise to transform the study of brain circuits in animal models and to decipher the structure–function relationships essential to understanding complex brain functions and their deficits in human brain disorders.

Acknowledgments

We thank Partha Mitra, Hongkui Zeng, and Christian Niedworok for comments on the manuscript and J. Kuhl for the graphics. P.O. is supported by National Institute of Mental Health Grant 1R01MH096946-01 and Simons Foundation for Autism Research Grants 204719 and 253447. T.W.M. is a Wellcome Trust Investigator and is supported by the Medical Research Council MC U1175975156. This chapter was previously published in full as Osten P, Margrie TW (2013) Mapping brain circuitry with a light microscope, *Nat Methods* 10:515–523.

References

- Ahrens MB, Keller PJ (2013) Whole-brain functional imaging at cellular resolution using light-sheet microscopy. *Nat Methods* 10:413–420.
- Ahrens MB, Li JM, Orger MB, Robson DN, Schier AF, Engert F, Portugues R (2012) Brain-wide neuronal dynamics during motor adaptation in zebrafish. *Nature* 485:471–477.
- Akerboom J, Chen TW, Wardill TJ, Tian L, Marvin JS, Mutlu S, Calderón NC, Esposti F, Borghuis BG, Sun XR, Gordus A, Orger MB, Portugues R, Engert F, Macklin JJ, Filosa A, Aggarwal A, Kerr RA, Takagi R, Kracun S, et al. (2012) Optimization of a GCaMP calcium indicator for neural activity imaging. *J Neurosci* 32:13819–13840.
- Alivisatos AP, Chun M, Church GM, Deisseroth K, Donoghue JP, Greenspan RJ, McEuen PL, Roukes ML, Sejnowski TJ, Weiss PS, Yuste R (2013) Neuroscience. The brain activity map. *Science* 339:1284–1285.
- Angelo K, Rancz EA, Pimentel D, Hundahl C, Hannibal J, Fleischmann A, Pichler B, Margrie TW (2012) A biophysical signature of network affiliation and sensory processing in mitral cells. *Nature* 488:375–378.
- Arenkiel BR, Hasegawa H, Yi JJ, Larsen RS, Wallace ML, Philpot BD, Wang F, Ehlers MD (2011) Activity-induced remodeling of olfactory bulb microcircuits revealed by monosynaptic tracing. *PLoS ONE* 6:e29423.
- Atasoy D, Aponte Y, Su HH, Sternson SM (2008) A FLEX switch targets channelrhodopsin-2 to multiple cell types for imaging and long-range circuit mapping. *J Neurosci* 28:7025–7030.
- Barth AL, Gerkin RC, Dean KL (2004) Alteration of neuronal firing properties after *in vivo* experience in a FosGFP transgenic mouse. *J Neurosci* 24:6466–6475.
- Beier KT, Saunders A, Oldenburg IA, Miyamichi K, Akhtar N, Luo L, Whelan SP, Sabatini B, Cepko CL (2011) Anterograde or retrograde transsynaptic labeling of CNS neurons with vesicular stomatitis virus vectors. *Proc Natl Acad Sci USA* 108:15414–15419.
- Bock DD, Lee WC, Kerlin AM, Andermann ML, Hood G, Wetzel AW, Yurgenson S, Soucy ER, Kim HS, Reid RC (2011) Network anatomy and *in vivo* physiology of visual cortical neurons. *Nature* 471:177–182.
- Bohland JW, Wu C, Barbas H, Bokil H, Bota M, Breiter HC, Cline HT, Doyle JC, Freed PJ, Greenspan RJ, Haber SN, Hawrylycz M, Herrera DG, Hilgetag CC, Huang ZJ, Jones A, Jones EG, Karten HJ, Kleinfeld D, Kötter R, et al. (2009) A proposal for a coordinated effort for the determination of brainwide neuroanatomical connectivity in model organisms at a mesoscopic scale. *PLoS Comput Biol* 5:e1000334.8
- Briggman KL, Helmstaedter M, Denk W (2011) Wiring specificity in the direction-selectivity circuit of the retina. *Nature* 471:183–188.
- Callaway EM (2008) Transneuronal circuit tracing with neurotropic viruses. *Curr Opin Neurobiol* 18:617–623.
- Chung K, Deisseroth K (2013) CLARITY for mapping the nervous system. *Nat Methods* 10:508–513
- Chung K, Wallace J, Kim SY, Kalyanasundaram S, Andalman AS, Davidson TJ, Mirzabekov JJ, Zalocusky KA, Mattis J, Denisin AK, Pak S, Bernstein H, Ramakrishnan C, Grosenick L, Gradinaru V, Deisseroth K (2013) Structural and molecular interrogation of intact biological systems. *Nature* 497:332–337.
- Conte WL, Kamishina H, Reep RL (2009) Multiple neuroanatomical tract-tracing using fluorescent Alexa Fluor conjugates of cholera toxin subunit B in rats. *Nat Protoc* 4:1157–1166.
- Craddock RC, Jbabdi S, Yan CG, Vogelstein JT, Castellanos FX, Di Martino A, Kelly C, Heberlein K, Colcombe S, Milham M (2013) Imaging human connectomes at the macroscale. *Nat Methods* 10:524–539.

- Defelipe J, López-Cruz PL, Benavides-Piccione R, Bielza C, Larrañaga P, Anderson S, Burkhalter A, Cauli B, Fairén A, Feldmeyer D, Fishell G, Fitzpatrick D, Freund TF, González-Burgos G, Hestrin S, Hill S, Hof PR, Huang J, Jones EG, Kawaguchi Y, et al. (2013) New insights into the classification and nomenclature of cortical GABAergic interneurons. *Nat Rev Neurosci* 14:202–216.
- Denk W, Strickler JH, Webb WW (1990) Two-photon laser scanning fluorescence microscopy. *Science* 248:73–76.
- Dotz HU, Leischner U, Schierloh A, Jährling N, Mauch CP, Deininger K, Deussing JM, Eder M, Zieglgänsberger W, Becker K (2007) Ultramicroscopy: three-dimensional visualization of neuronal networks in the whole mouse brain. *Nat Methods* 4:331–336.
- Dong HW (2008) The Allen reference atlas: a digital color brain atlas of the C57Bl/6J male mouse. Hoboken, NJ: Wiley.
- Ekstrand MI, Enquist LW, Pomeranz LE (2008) The alpha-herpesviruses: molecular pathfinders in nervous system circuits. *Trends Mol Med* 14:134–140.
- Emes RD, Grant SG (2012) Evolution of synapse complexity and diversity. *Ann Rev Neurosci* 35:111–131.
- Etessami R, Conzelmann KK, Fadai-Ghotbi B, Natelson B, Tsiang H, Ceccaldi PE (2000) Spread and pathogenic characteristics of a G-deficient rabies virus recombinant: an *in vitro* and *in vivo* study. *J Gen Virol* 81:2147–2153.
- Ewald AJ, McBride H, Reddington M, Fraser SE, Kerschmann R (2002) Surface imaging microscopy, an automated method for visualizing whole embryo samples in three dimensions at high resolution. *Dev Dyn* 225:369–375.
- Federspiel MJ, Bates P, Young JA, Varmus HE, Hughes SH (1994) A system for tissue-specific gene targeting: transgenic mice susceptible to subgroup A avian leukosis virus-based retroviral vectors. *Proc Natl Acad Sci USA* 91:11241–11245.
- Felleman DJ, Van Essen DC (1991) Distributed hierarchical processing in the primate cerebral cortex. *Cereb Cortex* 1:1–47.
- Fenko L, Yizhar O, Deisseroth K (2011) The development and application of optogenetics. *Ann Rev Neurosci* 34:389–412.
- Finke S, Conzelmann KK (2005) Replication strategies of rabies virus. *Virus Res* 111:120–131.
- Gerfen CR, Sawchenko PE (1984) An anterograde neuroanatomical tracing method that shows the detailed morphology of neurons, their axons and terminals: immunohistochemical localization of an axonally transported plant lectin, *Phaseolus vulgaris* leucoagglutinin (PHA-L). *Brain Res* 290:219–238.
- Glover JC, Petursdottir G, Jansen JK (1986) Fluorescent dextran-amines used as axonal tracers in the nervous system of the chicken embryo. *J Neurosci Methods* 18:243–254.
- Golgi C (1873) Sulla struttura della sostanza grigia del cervello. *Gazz Med Ital (Lombardia)* 33:244–246.
- Gong H, Zeng S, Yan C, Lv X, Yang Z, Xu T, Feng Z, Ding W, Qi X, Li A, Wu J, Luo Q (2013) Continuously tracing brain-wide long-distance axonal projections in mice at a one-micron voxel resolution. *Neuroimage* 74:87–98.
- Grinevich V, Brecht M, Osten P (2005) Monosynaptic pathway from rat vibrissa motor cortex to facial motor neurons revealed by lentivirus-based axonal tracing. *J Neurosci* 25:8250–8258.
- Grinevich V, Kollerker A, Eliava M, Takada N, Takuma H, Fukazawa Y, Shigemoto R, Kuhl D, Waters J, Seeburg PH, Osten P (2009) Fluorescent Arc/Arg3.1 indicator mice: a versatile tool to study brain activity changes *in vitro* and *in vivo*. *J Neurosci Methods* 184:25–36.
- Harris JA, Wook Oh S, Zeng H (2012) Adeno-associated viral vectors for anterograde axonal tracing with fluorescent proteins in nontransgenic and cre driver mice. *Curr Prot Neurosci* (Crawley JN, et al., eds.), Chap 1, Unit 1.20, pp. 21–18.
- Harvey CD, Collman F, Dombeck DA, Tank DW (2009) Intracellular dynamics of hippocampal place cells during virtual navigation. *Nature* 461:941–946.
- Harvey CD, Coen P, Tank DW (2012) Choice-specific sequences in parietal cortex during a virtual-navigation decision task. *Nature* 484:62–68.
- Hawrylycz M, Baldock RA, Burger A, Hashikawa T, Johnson GA, Martone M, Ng L, Lau C, Larson SD, Nissanov J, Puellas L, Ruffins S, Verbeek F, Zaslavsky I, Boline J (2011) Digital atlas and standardization in the mouse brain. *PLoS Comput Biol* 7:e1001065.
- Helmstaedter M (2013) Cellular-resolution connectomics: challenges of dense neural circuit reconstruction. *Nat Methods* 10:501–507.
- Herrera DG, Robertson HA (1996) Activation of c-fos in the brain. *Prog Neurobiol* 50:83–107.

NOTES

- Hintiryan H, Gou L, Zingg B, Yamashita S, Lyden HM, Song MY, Grewal AK, Zhang X, Toga AW, Dong HW (2012) Comprehensive connectivity of the mouse main olfactory bulb: analysis and online digital atlas. *Front Neuroanat* 6:30.
- Holmgren C, Harkany T, Svennenfors B, Zilberter Y (2003) Pyramidal cell communication within local networks in layer 2/3 of rat neocortex. *J Physiol* 551:139–153.
- Huber D, Gutnisky DA, Peron S, O'Connor DH, Wiegert JS, Tian L, Oertner TG, Looger LL, Svoboda K (2012) Multiple dynamic representations in the motor cortex during sensorimotor learning. *Nature* 484:473–478.
- Huisken J, Swoger J, Del Bene F, Wittbrodt J, Stelzer EH (2004) Optical sectioning deep inside live embryos by selective plane illumination microscopy. *Science* 305:1007–1009.
- Jones EG, Stone JM, Karten HJ (2011) High-resolution digital brain atlases: a Hubble telescope for the brain. *Ann NY Acad Sci* 1225(Suppl 1):E147–E159.
- Kalchmair S, Jahrling N, Becker K, Dodt HU (2010) Image contrast enhancement in confocal ultramicroscopy. *Opt Lett* 35:79–81.
- Keller PJ, Schmidt AD, Santella A, Khairy K, Bao Z, Wittbrodt J, Stelzer EH (2010) Fast, high-contrast imaging of animal development with scanned light sheet-based structured-illumination microscopy. *Nat Methods* 7:637–642.
- Kitamura K, Judkewitz B, Kano M, Denk W, Hausser M (2008) Targeted patch-clamp recordings and single-cell electroporation of unlabeled neurons *in vivo*. *Nat Methods* 5:61–67.
- Klausberger T, Somogyi P (2008) Neuronal diversity and temporal dynamics: the unity of hippocampal circuit operations. *Science* 321:53–57.
- Ko H, Hofer SB, Pichler B, Buchanan KA, Sjöström PJ, Mrsic-Flogel TD (2011) Functional specificity of local synaptic connections in neocortical networks. *Nature* 473:87–91.
- Koch C, Reid RC (2012) Neuroscience: observatories of the mind. *Nature* 483:397–398.
- Lanciego JL, Wouterlood FG (2011) A half century of experimental neuroanatomical tracing. *J Chem Neuroanat* 42:157–183.
- Lein ES, Hawrylycz MJ, Ao N, Ayres M, Bensinger A, Bernard A, Boe AF, Boguski MS, Brockway KS, Byrnes EJ, Chen L, Chen L, Chen TM, Chin MC, Chong J, Crook BE, Czaplinska A, Dang CN, Datta S, Dee NR, et al. (2007) Genome-wide atlas of gene expression in the adult mouse brain. *Nature* 445:168–176.
- Leischner U, Zieglgansberger W, Dodt HU (2009) Resolution of ultramicroscopy and field of view analysis. *PLoS ONE* 4:e5785.
- Li A, Gong H, Zhang B, Wang Q, Yan C, Wu J, Liu Q, Zeng S, Luo Q (2011) Micro-optical sectioning tomography to obtain a high-resolution atlas of the mouse brain. *Science* 330:1404–1408.
- Llewellyn-Smith IJ, Martin CL, Arnolda LF, Minson JB (2000) Tracer-toxins: cholera toxin B-saporin as a model. *J Neurosci Methods* 103:83–90.
- Lo L, Anderson DJ (2011) A Cre-dependent, anterograde transsynaptic viral tracer for mapping output pathways of genetically marked neurons. *Neuron* 72:938–950.
- Madisen L, Zwingman TA, Sunkin SM, Oh SW, Zariwala HA, Gu H, Ng LL, Palmiter RD, Hawrylycz MJ, Jones AR, Lein ES, Zeng H (2010) A robust and high-throughput Cre reporting and characterization system for the whole mouse brain. *Nat Neurosci* 13:133–140.
- Madisen L, Mao T, Koch H, Zhuo JM, Berenyi A, Fujisawa S, Hsu YW, Garcia AJ 3rd, Gu X, Zanella S, Kidney J, Gu H, Mao Y, Hooks BM, Boyden ES, Buzsáki G, Ramirez JM, Jones AR, Svoboda K, Han X, et al. (2012) A toolbox of Cre-dependent optogenetic transgenic mice for light-induced activation and silencing. *Nat Neurosci* 15:793–802.
- Mank M, Santos AF, Drenth S, Mrsic-Flogel TD, Hofer SB, Stein V, Hendel T, Reiff DF, Levelt C, Borst A, Bonhoeffer T, Hübener M, Griesbeck (2008) A genetically encoded calcium indicator for chronic *in vivo* two-photon imaging. *Nat Methods* 5:805–811.
- Margrie TW, Meyer AH, Caputi A, Monyer H, Hasan MT, Schaefer AT, Denk W, Brecht M (2003) Targeted whole-cell recordings in the mammalian brain *in vivo*. *Neuron* 39:911–918.
- Marshall JH, Mori T, Nielsen KJ, Callaway EM (2010) Targeting single neuronal networks for gene expression and cell labeling *in vivo*. *Neuron* 67:562–574.

- Mayerich D, Abbott L, McCormick B (2008) Knife-edge scanning microscopy for imaging and reconstruction of three-dimensional anatomical structures of the mouse brain. *J Microsc* 231:134–143.
- Mertz J, Kim J (2010) Scanning light-sheet microscopy in the whole mouse brain with HiLo background rejection. *J Biomed Opt* 15:016027.
- Meyer HS, Wimmer VC, Oberlaender M, de Kock CP, Sakmann B, Helmstaedter M (2010) Number and laminar distribution of neurons in a thalamocortical projection column of rat vibrissal cortex. *Cereb Cortex* 20:2277–2286.
- Meyer HS, Schwarz D, Wimmer VC, Schmitt AC, Kerr JN, Sakmann B, Helmstaedter M (2011) Inhibitory interneurons in a cortical column form hot zones of inhibition in layers 2 and 5A. *Proc Natl Acad Sci USA* 108:16807–16812.
- Micheva KD, Smith SJ (2007) Array tomography: a new tool for imaging the molecular architecture and ultrastructure of neural circuits. *Neuron* 55:25–36.
- Micheva KD, Busse B, Weiler NC, O'Rourke N, Smith SJ (2010) Single-synapse analysis of a diverse synapse population: proteomic imaging methods and markers. *Neuron* 68:639–653.
- Miyamichi K, Amat F, Moussavi F, Wang C, Wickersham I, Wall NR, Taniguchi H, Tasic B, Huang ZJ, He Z, Callaway EM, Horowitz MA, Luo L (2011) Cortical representations of olfactory input by trans-synaptic tracing. *Nature* 472:191–196.
- Moene IA, Subramaniam S, Darin D, Leergaard TB, Bjaalie JG (2007) Toward a workbench for rodent brain image data: systems architecture and design. *Neuroinformatics* 5:35–58.
- Naumann T, Hartig W, Frotscher M (2000) Retrograde tracing with Fluoro-Gold: different methods of tracer detection at the ultrastructural level and neurodegenerative changes of back-filled neurons in long-term studies. *J Neurosci Methods* 103:11–21.
- Ng L, Bernard A, Lau C, Overly CC, Dong HW, Kuan C, Pathak S, Sunkin SM, Dang C, Bohland JW, Bokil H, Mitra PP, Puelles L, Hohmann J, Anderson DJ, Lein ES, Jones AR, Hawrylycz M (2009) An anatomic gene expression atlas of the adult mouse brain. *Nat Neurosci* 12:356–362.
- Niedworok CJ, Schwarz I, Ledderose J, Giese G, Conzelmann KK, Schwarz MK (2012) Charting monosynaptic connectivity maps by two-color light-sheet fluorescence microscopy. *Cell Rep* 2:1375–1386.
- Oberlaender M, de Kock CP, Bruno RM, Ramirez A, Meyer HS, Dercksen VJ, Helmstaedter M, Sakmann B (2012) Cell type-specific three-dimensional structure of thalamocortical circuits in a column of rat vibrissal cortex. *Cereb Cortex* 22:2375–2391.
- Odgaard A, Andersen K, Melsen F, Gundersen HJ (1990) A direct method for fast three-dimensional serial reconstruction. *J Microsc* 159:335–342.
- O'Rourke NA, Weiler NC, Micheva KD, Smith SJ (2012) Deep molecular diversity of mammalian synapses: why it matters and how to measure it. *Nat Rev Neurosci* 13:365–379.
- Osten P, Margrie TW (2013) Mapping brain circuitry with a light microscope. *Nat Methods* 10:515–523.
- Paxinos G, Franklin KB (2004) The mouse brain in stereotaxic coordinates. Gulf Professional Publishing.
- Petilla Interneuron Nomenclature Group, Ascoli GA, Alonso-Nanclares L, Anderson SA, Barrionuevo G, Benavides-Piccione R, Burkhalter A, Buzsáki G, Cauli B, Defelipe J, Fairén A, Feldmeyer D, Fishell G, Fregnac Y, Freund TF, Gardner D, Gardner EP, Goldberg JH, Helmstaedter M, Hestrin S, et al. (2008) Petilla terminology: nomenclature of features of GABAergic interneurons of the cerebral cortex. *Nat Rev Neurosci* 9:557–568.
- Ragan T, Sylvan JD, Kim KH, Huang H, Bahlmann K, Lee RT, So PT (2007) High-resolution whole organ imaging using two-photon tissue cytometry. *J Biomed Opt* 12:014015.
- Ragan T, Kadiri LR, Venkataraju KU, Bahlmann K, Sutin J, Taranda J, Arganda-Carreras I, Kim Y, Seung HS, Osten P (2012) Serial two-photon tomography for automated *ex vivo* mouse brain imaging. *Nat Methods* 9:255–258.
- Ramón Y Cajal S (1904) *Textura del sistema nervioso del hombre y de los vertebrados*. Vol 2. Nicholas Moya.
- Rancz EA, Franks KM, Schwarz MK, Pichler B, Schaefer AT, Margrie TW (2011) Transfection via whole-cell recording *in vivo*: bridging single-cell physiology, genetics and connectomics. *Nat Neurosci* 14:527–532.

NOTES

- Reid RC (2012) From functional architecture to functional connectomics. *Neuron* 75:209–217.
- Reijmers LG, Perkins BL, Matsuo N, Mayford M (2007) Localization of a stable neural correlate of associative memory. *Science* 317:1230–1233.
- Reiner A, Veenman CL, Medina L, Jiao Y, Del Mar N, Honig MG (2000) Pathway tracing using biotinylated dextran amines. *J Neurosci Methods* 103:23–37.
- Rockland KS, Pandya DN (1979) Laminar origins and terminations of cortical connections of the occipital lobe in the rhesus monkey. *Brain Res* 179:3–20.
- Sands GB, Gerneke DA, Hooks DA, Green CR, Smaill BH, Legrice IJ (2005) Automated imaging of extended tissue volumes using confocal microscopy. *Microsc Res Tech* 67:227–239.
- Song CK, Enquist LW, Bartness TJ (2005) New developments in tracing neural circuits with herpesviruses. *Virus Res* 111:235–249.
- Song S, Sjöström PJ, Reigl M, Nelson S, Chklovskii DB (2005) Highly nonrandom features of synaptic connectivity in local cortical circuits. *PLoS Biol* 3:e68.
- Sunkin SM, Ng L, Lau C, Dolbeare T, Gilbert TL, Thompson CL, Hawrylycz M, Dang C (2013) Allen Brain Atlas: an integrated spatio-temporal portal for exploring the central nervous system. *Nucleic Acids Res* 41:D996–D1008.
- Swanson LW, Bota M (2010) Foundational model of structural connectivity in the nervous system with a schema for wiring diagrams, connectome, and basic plan architecture. *Proc Natl Acad Sci USA* 107:20610–20617.
- Takato J, Nelson A, Zhou X, Bolton MM, Ehlers MD, Arenkiel BR, Mooney R, Wang F (2013) New modules are added to vibrissal premotor circuitry with the emergence of exploratory whisking. *Neuron* 77:346–360.
- Taniguchi H, He M, Wu P, Kim S, Paik R, Sugino K, Kvitsiani D, Fu Y, Lu J, Lin Y, Miyoshi G, Shima Y, Fishell G, Nelson SB, Huang ZJ (2011) A resource of Cre driver lines for genetic targeting of GABAergic neurons in cerebral cortex. *Neuron* 71:995–1013.
- Thompson RH, Swanson LW (2010) Hypothesis-driven structural connectivity analysis supports network over hierarchical model of brain architecture. *Proc Natl Acad Sci USA* 107:15235–15239.
- Thomson AM, West DC, Wang Y, Bannister AP (2002) Synaptic connections and small circuits involving excitatory and inhibitory neurons in layers 2–5 of adult rat and cat neocortex: triple intracellular recordings and biocytin labelling *in vitro*. *Cereb Cortex* 12:936–953.
- Tsai PS, Friedman B, Ifarraguerrri AI, Thompson BD, Lev-Ram V, Schaffer CB, Xiong Q, Tsien RY, Squier JA, Kleinfeld D (2003) All-optical histology using ultrashort laser pulses. *Neuron* 39:27–41.
- Tsai PS, Kaufhold JP, Blinder P, Friedman B, Drew PJ, Karten HJ, Lyden PD, Kleinfeld D (2009) Correlations of neuronal and microvascular densities in murine cortex revealed by direct counting and colocalization of nuclei and vessels. *J Neurosci* 29:14553–14570.
- Ugolini G (1995) Specificity of rabies virus as a transneuronal tracer of motor networks: transfer from hypoglossal motoneurons to connected second-order and higher order central nervous system cell groups. *J Comp Neurol* 356:457–480.
- Ugolini G (2010) Advances in viral transneuronal tracing. *J Neurosci Methods* 194:2–20.
- Wall NR, Wickersham IR, Cetin A, De La Parra M, Callaway EM (2010) Monosynaptic circuit tracing *in vivo* through Cre-dependent targeting and complementation of modified rabies virus. *Proc Natl Acad Sci USA* 107:21848–21853.
- Wallace DJ, Meyer zum Alten Borgloh S, Astori S, Yang Y, Bausen M, Kügler S, Palmer AE, Tsien RY, Sprengel R, Kerr JN, Denk W, Hasan MT (2008) Single-spike detection *in vitro* and *in vivo* with a genetic Ca²⁺ sensor. *Nat Methods* 5:797–804.
- Wickersham IR, Feinberg EH (2012) New technologies for imaging synaptic partners. *Curr Opin Neurobiol* 22:121–127.
- Wickersham IR, Finke S, Conzelmann KK, Callaway EM (2007a) Retrograde neuronal tracing with a deletion-mutant rabies virus. *Nat Methods* 4:47–49.
- Wickersham IR, Lyon DC, Barnard RJ, Mori T, Finke S, Conzelmann KK, Young JA, Callaway EM (2007b) Monosynaptic restriction of transsynaptic tracing from single, genetically targeted neurons. *Neuron* 53:639–647.
- Young JA, Bates P, Varmus HE (1993) Isolation of a chicken gene that confers susceptibility to infection by subgroup A avian leukosis and sarcoma viruses. *J Virol* 67:1811–1816.